

## 非対称下型電極を用いた共振型光変調器の設計と特性評価

川西哲也<sup>†</sup> 及川哲<sup>††</sup> 日限薫<sup>††</sup> 松尾善郎<sup>†</sup> 井筒雅之<sup>†</sup>

† 通信総合研究所

〒184-8795 東京都小金井市貫井北町4-2-1

†† 住友大阪セメント(株)新規技術研究所

〒274-8601 千葉県船橋市豊富585

E-mail: †kawanish@crl.go.jp

あらまし 非対称下型共振電極を用いた帯域動作型LiNbO<sub>3</sub>光変調器を規格化誘導位相量を最大化する電極長を求めるとい  
う手法で設計し、試作した。非対称下型電極は長さおよび終端方法の異なる2つの変調電極からなる。電極長が1.76mmで、  
6.2GHzにおいて規格化誘導位相量4.96を得た。

キーワード 光変調器, 共振, 非対称下型電極, 導波路, インピーダンス整合

## Design and Estimation of LiNbO<sub>3</sub> Optical Modulator with an Asymmetric Resonant Structure

Tetsuya KAWANISHI<sup>†</sup>, Satoshi OIKAWA<sup>††</sup>, Kaoru HIGUMA<sup>††</sup>, Yoshiro MATSUO<sup>†</sup>, and Masayuki  
IZUTSU<sup>†</sup>

† Communications Research Laboratory

4-2-1 Nukui-Kitamachi, Koganei, Tokyo 184-8795, Japan

†† New Technology Research Laboratories, Sumitomo Osaka Cement

585 Toyotomi, Funabashi, Chiba 274-8601, Japan

E-mail: †kawanish@crl.go.jp

**Abstract** LiNbO<sub>3</sub> optical modulators for band-operation with a resonant modulating electrode are investigated in this  
paper. We propose an asymmetric resonant structure consisting of two arms of modulating electrodes, where one arm is  
open-ended and the other arm is short-ended. The optical response at 6.2 GHz of a resonant modulator designed by  
maximizing the normalized induced phase was 4.94 of the response at dc with a non-resonant modulator.

**Key words** optical modulator, resonance, asymmetric structure, waveguide, impedance matching

## 1 Introduction

High-speed optical modulators are key devices used in wide-band communication systems. In conventional modulators, traveling-wave electrodes are used to achieve broad-band optical response up to the millimeter wave region [1, 2, 3, 4]. The velocity of an electric guided wave on a traveling-wave electrode matches that of a lightwave propagating in an optical waveguide. The electric field induced by the guided wave can interact with the lightwave, while the guided wave propagates on the electrode. Thus, the interaction can be enhanced by using a long traveling-wave electrode in the broadband region (ex. dc-40 GHz). On the other hand, band-operation optical modulators are required in radio-on-fiber systems [5, 6]. By using resonant structures, we can obtain effective optical modulation in a particular band [7, 8, 9].

The voltage on the modulating electrode can be enhanced by the resonance of transmission lines, which increases the efficiency of the optical modulation even with a short electrode. If the feeding point of the modulating electrode is close to the node of the standing-wave voltage profile, the peak voltage on the electrode is much higher than the voltage at the feeding point. However, the impedance at the feeding point is low, so that the voltage at the feeding point is also low. Thus, the peak voltage is low in relation to the input voltage. To enhance the peak voltage, it is necessary to increase the impedance at the feeding point, while keeping the feeding point, close to the node of the standing wave. Sasaki and Izutsu (1997) proposed an optical modulator for band-operation. It consisted of two resonant electrodes with a patch capacitance at the feeding point [10]. The two electrodes were the same length; they were slightly longer than one-quarter or three-quarters of the wavelength propagating on the electrode. The impedance of the electrodes is inductive and very small. The patch capacitance was designed to match the impedance at the feeding point, between the feeding line and the combined impedance of the electrodes and the capacitance. However, the modulator described in the previous work is difficult to make because its patch capacitance consisted of a complicated three-dimensional structure. In the work described in this paper, we investigated a resonant-type Mach-Zehnder optical modulator

consisting of planar structures, designed to overcome the problems of making such a device and to increase the efficiency of the optical modulation.

## 2 Asymmetric resonant structure

As shown in Fig. 1, the modulating electrode has two arms that are asymmetric coplanar waveguides (ACPWs). The ground plane, modulating electrode, and feeding line consist of gold whose thickness is  $t_{EL}$ , where  $s$  is the width of the gap between the ground plane and the modulating electrode, and  $\omega$  is the width of the modulating electrode. The feeding line, which is connected at the junction of the two arms, is a coplanar waveguide. A buffer layer, whose thickness is  $t_{BUF}$ , is there to reduce the loss of the lightwave propagating in the optical waveguides under the metal electrodes. The short arm (Arm I), with length denoted by  $L_1$ , is short-ended, while the long arm (Arm II), with length denoted by  $L_2$ , is open-ended. The two arms differ in length and termination, so that we termed this configuration the asymmetric resonant structure. The equivalent circuit is shown in Fig. 2, where the impedance of Arm I ( $Z_1$ ) and that of Arm II ( $Z_2$ ) are expressed by

$$Z_1 = Z_0 \tanh \gamma L_1 \quad (1)$$

$$Z_2 = Z_0 \coth \gamma L_2. \quad (2)$$

$Z_0$  is the characteristic impedance of ACPW.  $\gamma (= \alpha + j\beta)$  denotes the propagation coefficient. The total impedance of the asymmetric resonant structure is given by

$$Z_L = Z_0 \frac{\tanh \gamma L_1 \coth \gamma L_2}{\tanh \gamma L_1 + \coth \gamma L_2} \quad (3)$$

The voltage on the modulating electrode is given by

$$V(y, t) = \text{Re} \left[ TG(y) V_{in} e^{j2\pi f(t-t_0)} \right], \quad (4)$$

where  $V_{in} e^{j2\pi f(t-t_0)}$  is the input voltage whose frequency is  $f$ . For simplicity, we assume  $V_{in} = 1$ . The voltage transmittance at the junction is defined by

$$T \equiv \frac{2Z_L}{Z_L + Z_f}, \quad (5)$$

where  $Z_f$  is the characteristic impedance of the feeding line.  $|T|$  is an increasing function of  $|Z_L|$ , and the range is from 0 ( $|Z_L| = 0$ ) to 2 ( $|Z_L| = \infty$ ).

$G(y)$  expresses the distribution of the standing voltage wave on the electrode and is defined by

$$G(y) \equiv \begin{cases} \frac{\cosh \gamma(L_2 - y)}{\cosh \gamma L_2} & (y > 0) \\ \frac{\sinh \gamma(L_1 + y)}{\sinh \gamma L_1} & (y < 0) \end{cases} \quad (6)$$

The induced phase at each optical waveguide is the sum of the Pockels effect with respect to the coordinate system moving along with the lightwave propagating in the optical waveguide. Thus, the difference of the induced phases of the two optical waveguides of the Mach-Zehnder structure can be expressed by

$$\phi = \frac{\pi}{\lambda_0} n_0^3 r_{33} \frac{\Gamma}{s} L \Phi \quad (7)$$

$$\Phi \equiv \frac{1}{L} \int_{-L_1}^{L_2} V(y, \frac{y}{c} n_0 + t) dy, \quad (8)$$

where  $c$  is the speed of light.  $\lambda_0$  and  $n_0$  are the wavelength and refractive index of the lightwave, respectively.  $L \equiv L_1 + L_2$  is the total length of the modulating electrodes.  $\Gamma$  is the overlap integral between the field of the lightwave and the field induced by the electrode. The Pockels effect between the  $z$ -direction component of the electric field induced by the modulating electrode and lightwave whose electric field is polarized in the  $z$ -direction is considered, because the electrooptic coefficient of the effect mentioned above ( $r_{33}$ ) is the largest one. The factor of  $\frac{y}{c} n_0 + t$  means the phase difference due to the propagation delay of the lightwave.

The integral of the voltage on the electrode defined by Eq. (8),  $\Phi$ , is termed normalized induced phase, and shows the effect, of the resonant structure. The normalized induced phase for an optical modulator with a resonant structure can be larger than unity, while the normalized induced phase for a lossless perfectly velocity-matched traveling wave modulator equals unity. The half-wave voltage of the modulator  $V_{\pi}$  is given by  $\pi/\phi$ . Similarly,  $V_{\pi} L$ , defined by  $\pi L/\phi$  ( $\propto \Phi^{-1}$ ), is the voltage-length product which shows the degree of the modulation efficiency and the scale of the modulator. To obtain compact and effective optical modulators for band-operation, we designed them to have large normalized induced phases, as shown in following sections.

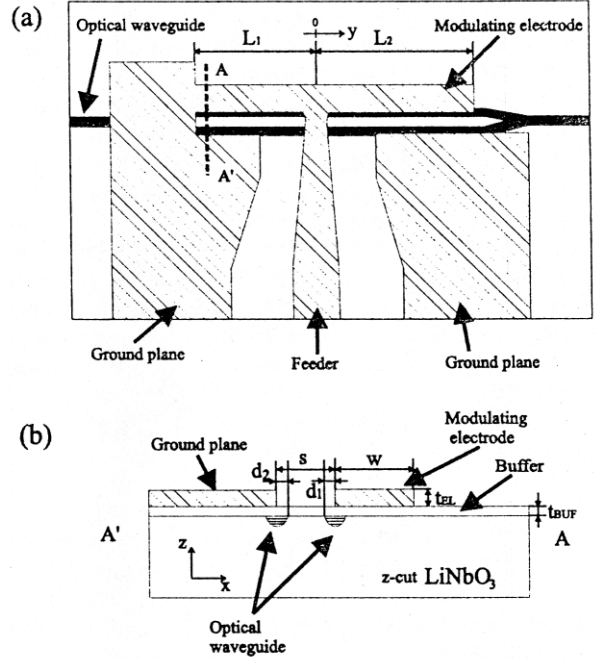


Figure 1: Structure of an optical modulator with an asymmetric resonant structure. (a) top view, (b) cross-section.

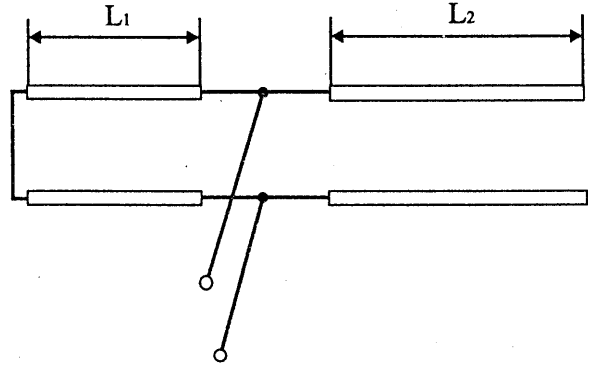


Figure 2: Equivalent circuit for the asymmetric resonant electrode.

$w[\mu\text{m}]$	$\alpha[1/\text{m}]$	$\beta[\text{rad}/\text{m}]$	$Z_0[\Omega]$
5	25.92	735.2	70.10
10	21.16	808.0	55.68
20	16.54	851.9	45.22
50	11.24	891.8	34.71

Table 1 : Dependence of the propagating constant and the characteristic impedance of the modulating electrode on the width of the electrode.

### 3 DeSign by maximizing the normalized induced phase

We consider a ACPW with the following:  $t_{BUF} = 0.55 \mu\text{m}$ ,  $s = 27 \mu\text{m}$ , and  $t_{EL} = 2 \mu\text{m}$ . Dependence of  $\gamma$  and  $Z_0$  on  $\omega$  at 10 GHz was calculated by using an electro-magnetic field calculator with the finite element method (HP-HFSS5.4), as shown in Table 1. To reduce the loss  $\alpha$ ,  $\omega$  was set to be  $50 \mu\text{m}$ . Thus, the wavelength of a 10 GHz Voltage wave on the ACPW ( $\lambda = 2\pi/\beta$ ) was 7.03 mm. The following parameters were used for numerical calculations:  $\epsilon_{SiO_2} = 4.0$ ,  $\epsilon_{LiNbO_3[xy]} = 43.0$ ,  $\epsilon_{LiNbO_3[z]} = 28.0$  and  $\sigma_{Au} = 4.3 \times 10^7 (\Omega\text{m})^{-1}$ .  $\epsilon_{LiNbO_3[xy]}$  and  $\epsilon_{LiNbO_3[z]}$  denote permittivities of  $LiNbO_3$  in the  $xy$ -plane and the  $z$ -direction, respectively.  $\epsilon_{SiO_2}$  and  $\sigma_{Au}$  are permittivity of the buffer layer ( $SiO_2$ ) and conductivity of the electrodes ( $Au$ ), respectively.

By using Eqs. (7) and (8), we obtained a combination of  $L_1$  and  $L_2$ , which gave a maximum of  $\Phi$ . When  $L_1 = 0.03\lambda$  and  $L_2 = 0.22\lambda$ ,  $\Phi$  had a maximum of 3.7 at 10 GHz. Fig. 3 shows the normalized induced phase as a function of the frequency  $f$ . In addition to a peak at 10 GHz, there are peaks due to high-order resonance at 30 and 50 GHz. In Fig. 4, the voltage reflectivity at the junction and the total impedance of these two modulating electrodes were shown as functions of  $f$ . The denominator of Eq. (3) goes to a minimum at resonance, which corresponds to parallel resonance of the two arms, so that the impedance has peaks at the resonant frequencies (10, 30, 50, and 70 GHz). As shown in Fig. 4, the reflectivity has dips, where the impedance has peaks. The peaks of the optical response were caused by enhancement of  $T$ .

If both arms were terminated by the same impedance (e.g. open or short), the polarity of the standing-wave voltage profile would change on the electrodes and the length  $L_1$  or  $L_2$  should be longer to obtain the resonance. In an asymmetric resonant structure, however, both  $L_1$  and  $L_2$  are smaller than a quarter of the wavelength  $\lambda$ . As shown in Fig. 5, the polarity does not change, which is why an asymmetric structure can reduce the half-wave voltage and the electrode length. At the end of Arm II, the voltage amplitude is approximately six times as large as the input voltage. The length of Arm II is slightly shorter than  $\lambda/4$ , so that Arm II is nearly in resonance and that the impedance of Arm II is

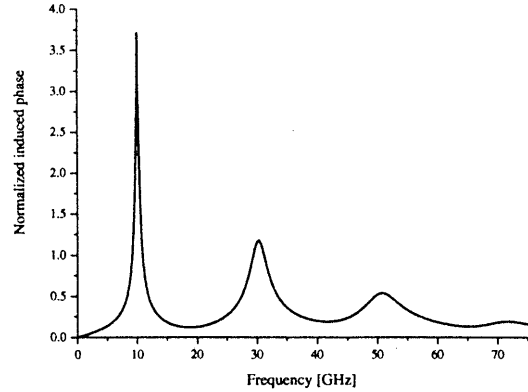


Figure 3: Optical response of a designed modulator, where  $L_1 = 0.03\lambda$  and  $L_2 = 0.22\lambda$ .

small. But, the total impedance  $Z_L$  is large owing to Arm I which has two functions: as a stub to enhance the impedance and as a modulating electrode. Arms I and II are in parallel resonance, where Arm I is capacitive and Arm II is inductive. In addition, the resonance can occur even when the length  $L_1$  or  $L_2$  are slightly varied, as shown in Fig. 6.

### 4 Experimental results

We measured the optical and electrical response of a fabricated modulator having the following:  $t_{BUF} = 0.55 \mu\text{m}$ ,  $\omega = 50 \mu\text{m}$ ,  $s = 27 \mu\text{m}$ ,  $t_{EL} = 2 \mu\text{m}$ ,  $L_1 = 0.03\lambda = 0.21 \text{ mm}$  and  $L_2 = 0.22\lambda = 1.55 \text{ mm}$ . Thus, the total length  $L$  was 1.76 mm. The central inductor of the feeding line was  $50 \mu\text{m}$  wide and the characteristic impedance was  $50 \Omega$ . The Mach-Zehnder interferometer consisted of two optical waveguides formed by the titanium diffusion technique on a  $z$ -cut  $LiNbO_3$  substrate. The refractive index  $n_0$  was assumed to be 2.2 for  $\lambda_0 = 1.55 \mu\text{m}$ . The effective width and depth of the optical waveguides were  $10 \mu\text{m}$  and  $8 \mu\text{m}$ , respectively. The positions of the waveguides were as follows:  $d_1 = 2 \mu\text{m}$  and  $d_2 = 3 \mu\text{m}$ . The overlap integral  $\Gamma$ , calculated by TEM approximation [11], was 0.92, where the thickness of the electrode  $t_{EL}$  was neglected. The profile of the mode guided in the optical waveguide was elliptic and the field distribution was assumed to be uniform. The modulator also had an open-ended dc-bias electrode to set

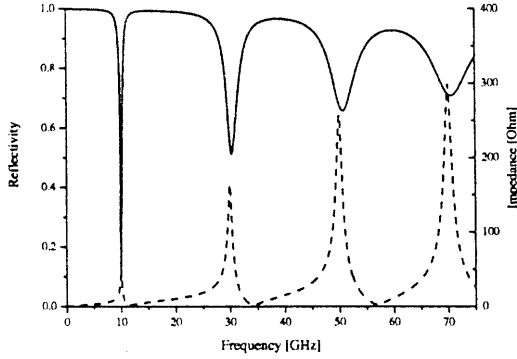


Figure 4: Electric response of a designed modulator. Solid line and dashed line denote voltage reflectivity at the junction and impedance of the asymmetric resonant structure, respectively, where  $L_1 = 0.03\lambda$  and  $L_2 = 0.22\lambda$ .

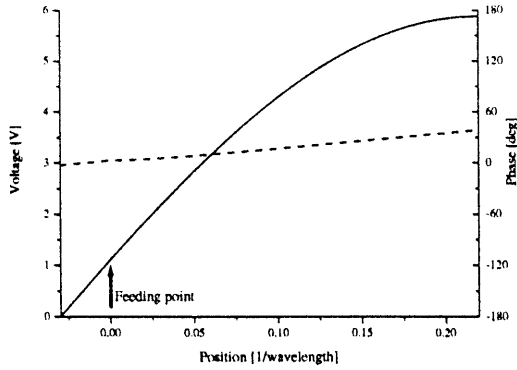


Figure 5: Voltage wave distribution on modulating electrodes, with respect to the coordinate system moving along with the lightwave propagating in the optical waveguide  $V(y, \frac{y}{c} n_0 + t)$ . Solid line and dashed line denote the amplitude and the phase of the voltage wave, respectively.

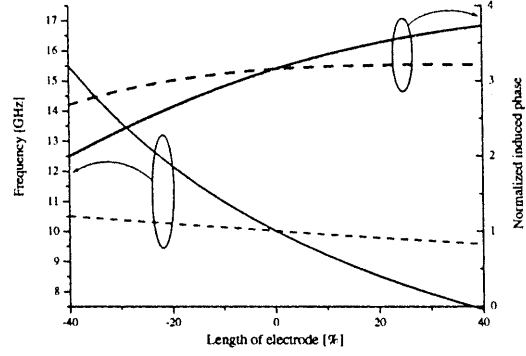


Figure 6: Dependence of the optical response on the lengths of the modulating electrodes. Solid lines denote the resonant frequency of the optical response and the induced phase at the resonance as functions of variation of  $L_1$ . Dashed lines show the resonant frequency and the induced phase as functions of variation of  $L_2$ .

the Mach-Zehnder switch function to the quadrature point. The normalized induced phase can be measured as the ratio of the optical response of a resonant electrode at a particular frequency to that of a non-resonant electrode at dc, where both electrodes were the same length.  $\Gamma$  obtained by the response measured at dc was 0.82, which was 89% of the calculated one. This discrepancy was due to the effect of the thickness of the electrode or deformation of the lightwave field pattern. As shown in Fig. 7, the optical response for the 1.55- $\mu\text{m}$  region, obtained from the responses of the resonant and dc-bias electrodes, had a peak of 4.94 at 6.2 GHz. The halfwave-voltage was 17.9 V at the peak. The fitting curve was obtained by changing the propagation constant  $\gamma$  from the numerically obtained one.  $\gamma$  was set to be  $0.4\alpha + j1.6\beta$ , where  $\alpha$  and  $\beta$  are real and imaginary parts of numerically obtained propagation constant (see Table. 1). This result may be due to the difference between the numerically calculated wavenumber and the actual one, and to the deformation of the field at the junction. The measured electric response (reflectivity) is also shown in Fig. 7. There are three dips near the resonant, peak of the optical response. The dips at 5 GHz and 8 GHz may have been caused by a reflection at a connector or a junction.

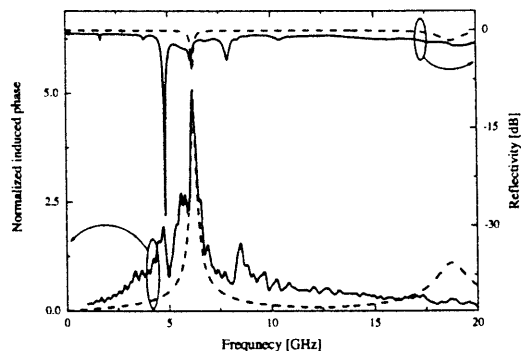


Figure 7: Responses of the fabricated modulator. Optical responses (normalized induced phase) and electric responses (reflectivity) are shown as functions of the frequency. Solid lines denote measured responses. Dashed lines denote the fitting curves.

## 5 Conclusion

An optical modulator with an asymmetric modulating electrode for band-operation was investigated. We proposed two design methods: maximizing the normalized induced phase and maximizing the peak voltage. The latter one is much simpler than the former one, but both methods gave the same result. The normalized induced phase of the fabricated modulator was 4.94. The half-wave voltage was 17.9 V in the 1.55- $\mu\text{m}$  wavelength range, in spite of the short electrode length of 1.76 mm.

## References

- [1] M. Izutsu, H. Haga and T. Sueta, 0 to 18 GHz traveling-wave optical waveguide intensity modulator, *IECE Trans.*, E63, 817-818 (1980)
- [2] O. Mitomi, K. Noguchi and H. Miyazawa, Design of ultra-broad-band LiNbO<sub>3</sub> optical modulators with ridge structure, *IEEE Trans. Micro. Theory Tech.* **43**, 2203-2207 (1995)
- [3] K. Noguchi, O. Mitomi and H. Miyazawa, Millimeter-wave Ti : LiNbO<sub>3</sub> optical modulators, *J. Lightwave Technol.* **16**, 615-619 (1998)
- [4] K. Noguchi, H. Miyazawa and O. Mitomi, 40-Gbit/s Ti : LiNbO<sub>3</sub> optical modulator with a two-stage electrode, *IEICE Trans.* **E81-C**, 1316-1320 (1998)
- [5] C. Lim, A. Nirmalathas, D. Novak and R. Waterhouse, Optimisation of baseband modulation scheme for millimetre-wave fibre-radio systems, *Electron. Lett.*, **36**, 442-443 (2000)
- [6] T. Kuri, K. Kitayama and Y. Takahashi, 60-GHz-Band Full-Duplex Radio-On-Fiber System Using Two-RF-Port Electroabsorption Transceiver, *IEEE Photonics Tech. Lett.*, **12**, 419-421 (2000)
- [7] Y. Zhou, M. Izutsu and T. Sueta, Low-Drive-Power Asymmetric Mach-Zehnder Modulator with Band-Limited Operation, *J. Lightwave Technol.*, **9**, 750-753 (1991)
- [8] K. Yoshida, A. Nomura and Y. Kanda, LiNbO<sub>3</sub> optical modulator using a superconducting resonant electrode, *IEICE Trans.*, **E77-C**, 1181-1184 (1994)
- [9] M. Izutsu, T. Mizuochi and T. Sueta, Band operation of guided-wave light modulators with filter-type coplanar electrodes, *IEICE Trans.*, **E78-C**, 55-60 (1995)
- [10] M. Sasaki and M. Izutsu, High-speed light modulator, *FST'97* (1997)
- [11] R. E. Collin, *Field Theory of Guided Waves*, 2nd ed., (IEEE Press, NY, 1991), 247-328